# Magnetostatic mode spectrum of rectangular ferromagnetic particles

P. H. Bryant

*Department of Physics, University of California, Berkeley, California 94720
and Materials Sciences Division, Lawrence Berkeley Laboratory, Berkeley, California 94720*

J. F. Smyth,* S. Schultz, and D. R. Fredkin

*Department of Physics, University of California, San Diego, La Jolla, California 92093*

Approximate methods for obtaining the magnetostatic mode spectrum of thin rectangular samples have been known for some time. However, our experimental results from lithographic arrays of submicron Permalloy particles show that these methods perform relatively poorly if the (in-plane) applied field is not large compared to $4\pi M_s$. We present an improved method for finding the spectrum that takes into account both the elliptical character of the mode precession and sample edge effects. We show that the case of an infinite magnetic strip can be reduced to a one-dimensional eigenvalue problem which we solve numerically, yielding insight into the more difficult rectangular case. Effects of the nonuniform demagnetization field on the spatial patterns and frequencies of the modes are also studied.

## I. INTRODUCTION

The spectrum of magnetostatic modes of magnetic particles of a particular shape are an important characteristic of those particles. A number of different geometries have been studied, and in some cases the theory provides exact analytic results, such as in the case of a spheroid,[1] an infinite slab,[2] or an infinite cylinder.[3] These "exact" results make assumptions about the sample, i.e., that any pinning of the surface spins may be neglected, the material is isotropic, the wavelength is large enough to justify neglecting exchange effects, and that the sample is uniformly magnetized and exhibits a uniform internal demagnetization field. In the case of thin rectangular particles things become more complicated and exact solutions cannot be found even under the above assumptions, some of which may no longer be reasonable, such as the uniformity of the demagnetization field and the magnetization. One may also wish to approximately determine the effect of exchange on the spectrum. The mode spectrum of rectangular particles has been examined by several authors[4,5] under a variety of approximations and assumptions. We seek here to improve in a number of ways on their results. In the process of examining this problem, we have also generated numerically the exact solution to a case not previously studied: the modes of an infinite thin strip with a dc field along its length. The general solution to this problem reduces to a one-dimensional eigenvalue problem. The results of this analysis give insight into the "edge effects" which also occur in the rectangular case. We also examine the effects of a nonuniform demagnetization field and of the sample thickness. The main motivation for conducting this study was to attempt to explain the resonance spectrum obtained from lithographically produced arrays of submicron rectangular Permalloy particles.[6] As we will show, the previously existing theories are very poor predictors of the observed spectra and can be greatly improved upon.

The previous studies can be generally grouped into two types, the variational method and the quantized slab method. In the variational method (see Sparks[4]) the modes are approximated as the eigenfunctions of a Hermitian operator. Using trial functions for the modes, approximate values for the mode frequencies can be determined. This approach includes exchange effects on the mode frequencies and provides analytic (though not exact) expressions for the mode frequencies. However, it produces errors resulting from noncircular precession of the magnetization, edge effects (due to finite sample geometry), nonuniformity of the demagnetization field and magnetization, and deviations of the true magnetization pattern from the chosen trial function. The quantized slab method (see Storey et al.[5]) uses the exact solutions for the infinite slab of Damon and Eshbach[2] and "quantizes" them by taking only those solutions which have periodicity that fits the dimensions of the sample. Since this method starts with an exact solution, it may do very well in cases where the edge effects are unimportant (high-order modes mainly). Some disadvantages are no corrections for edge effects, nonuniformity of demagnetization field or magnetization pattern, or exchange effects.

Our experimental results are obtained from lithographic arrays of submicron Permalloy particles, having $M_s \approx 800$ G. In Fig. 1 we show the experimental mode spectrum for a particular array consisting of approximately $10^5$ particles each 1 $\mu$m wide, 3 $\mu$m long, and 0.0735 $\mu$m thick. Permalloy, being a ferromagnetic metal, is subject to additional damping mechanisms that are due to the presence of conduction electrons.[7] However, we still obtain a relatively small linewidth of about 40 G, and there does not seem to be any reason to expect significant deviations in the frequencies or mode charac-
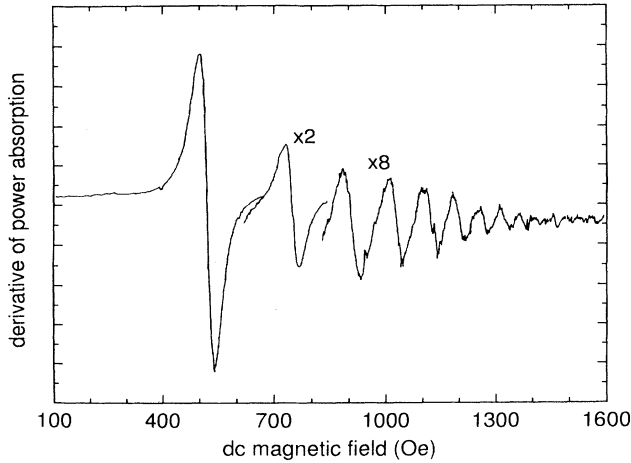
FIG. 1. Experimental data of the ferromagnetic resonance spectrum for an array of well-separated identical rectangular Permalloy particles. The particles are 1 $\mu$m$\times$3 $\mu$m$\times$0.0735 $\mu$m and the dc field was applied along the 3 $\mu$m direction. The resonances correspond to the excitation of magnetostatic modes. Portions of the figure labeled $\times$2 and $\times$8, were amplified vertically by these factors in order to improve the resolution of the smaller resonances.

teristics as a result of these effects. Another factor to consider in metals is the skin effect. This can have an influence on the coupling to the applied rf field, since it will create a nonuniform excitation field in the sample. Our samples are too thin for this to play an important role however. The spacing of the particles was approximately 6 $\mu$m which we believe is sufficient for them to behave as independent particles based on magnetization studies as a function of particle spacing. The sample was placed in a dc magnetic field aligned with the long axes of the particles and excited by perpendicular pumping with microwaves at 9.47 GHz. Qualitative comparison of Fig. 1 with previous studies of rectangular particles makes the determination of the mode indices reasonably certain in this case. From symmetry considerations, only modes with odd indices can be excited, these are the modes which are symmetric about the center of the particle along both the length and width of the particle. The first index, $n_y$, represents the number of half cycles along the length and the second, $n_x$, is the number along the width. The mode sequence in Fig. 1, from left to right is (1,1), (3,1), (5,1), (7,1), etc. The corresponding sequence of observed resonant fields is 520, 751, 911, 1034, 1128, 1202, 1273, 1330, 1382, etc. Using the variational method of Sparks[4] to calculate the internal field for resonance [see Sparks, Eq. (43c)], and then increasing this by the magnitude of the dc demagnetization field, which we will take here to be about 80 G, we obtain the sequence 1119, 1172, 1237, 1300, 1359, 1413, 1464, 1509, 1550, etc. Note that the calculated value of the field for the (1,1) mode is considerably too high and the spacing of the modes is is much smaller than the experimental values. As we will show the main source of error comes from the highly elliptical precession that occurs for our operating conditions. Ellipticity was much more moderate in

previous studies,[5,8-10] primarily done with yttrium iron garnet (YIG) films which have a considerably smaller saturation magnetization $M_s$ than does Permalloy. In these cases the Sparks formulas work quite well.

We will now proceed with our analysis of this problem, the theory being developed in Secs. II–V, with our most general result for the mode frequency being given by Eq. (46). Theory and experiment are then compared in Sec. VI, and found to be in very good agreement.

## II. INFINITE PLANE

As a first step in our analysis we consider the case of an infinite thin plane. The thickness $S$ is considered small enough that the magnetization is approximately constant across the thickness of the film. We take the internal dc field $H_i$ to lie in the plane along the $y$ axis. The $z$ axis is taken to be normal to the film. The modes will be taken to be small perturbations from the equilibrium state in which the magnetization is everywhere parallel to the $y$ axis and has the constant magnitude $M_s$. We find this problem has a standing wave solution. The small deviations $M_x$ and $M_y$ for a particular mode are

$$M_x = A_x F(x,y) \sin(\omega t), \tag{1}$$

$$M_z = A_z F(x,y) \cos(\omega t), \tag{2}$$

where

$$F(x,y) = \sin(k_x x) \sin(k_y y). \tag{3}$$

We find that this magnetic pattern produces a proportional magnetic field,

$$H_x = B_x F(x,y) \sin(\omega t), \tag{4}$$

$$H_z = B_z F(x,y) \cos(\omega t). \tag{5}$$

From the assumption that the mode wavelength is long compared to sample thickness we find

$$B_z/A_z = -4\pi. \tag{6}$$

The $x$ component of the magnetization also produces a magnetic charge distribution, which (per unit area of film) is

$$\sigma = -S\nabla \cdot M = -A_x k_x S \cos(k_x x) \sin(k_y y) \sin(\omega t). \tag{7}$$

By calculating the corresponding field we find that the ratio of the field to the magnetization in the $x$ direction is given by

$$B_x/A_x = -2\pi S k_x^2 / \sqrt{k_x^2 + k_y^2}. \tag{8}$$

To obtain the time dependence we start with the gyromagnetic equation

$$\dot{M} = -\gamma M \times H \tag{9}$$

where $\gamma \approx 1.76 \times 10^7$ sec$^{-1}$ G$^{-1}$ is the gyromagnetic ratio. A small signal analysis of this equation yields the following equations of motion:

$$\dot{M}_x = -\omega_z M_z, \tag{10}$$

$$\dot{M}_z = \omega_x M_x, \tag{11}$$

where

$$\omega_x = \gamma[-M_s B_x/A_x + H_i], \tag{12}$$
$$\omega_z = \gamma[-M_s B_z/A_z + H_i]. \tag{13}$$

From these equations we obtain the time dependence indicated previously with the frequency given by

$$\omega = \sqrt{\omega_x \omega_z} \tag{14}$$

and the $x$ to $z$ magnetization ratio given by

$$A_x/A_z = \sqrt{\omega_z/\omega_x}. \tag{15}$$

Thus we see that in cases where the values of $\omega_x$ and $\omega_z$ are quite different the magnetization will precess in a highly elliptical orbit.

These results could now be used to obtain approximate values for the case of a rectangular film by choosing only those solutions which are zero on the sample boundaries. One source of error in this approximation is edge effects which result from the fact that across the film in the $x$ direction the magnetization pattern stops abruptly at the edges unlike the infinite plane. We will study the edge effects by obtaining solutions to the problem of an infinite thin strip of finite width. "End effects" are another source of error which result from the nonuniformity of the dc demagnetization field which is generated by magnetic poles at the sample ends. We treat this effect for a long sample by making $k_y$ position dependent. Finally,

we correct for finite thickness of the sample using a variational approach similar to that used by Sparks.[4]

## III. INFINITE STRIP

We now consider the case of an infinite strip with the applied field along the infinite $y$ direction and the finite width of the strip extending in the $x$ direction from 0 to $W$. The thickness $S$ is assumed to be small. Solutions are found which have the same proportional form used previously [see Eqs. (1) and (4)] but with a different function $F(x,y)$. The ratio of the field to magnetization in the $z$ direction will still be $-4\pi$ as it was previously [Eq. (6)], all we need to do is to find magnetization patterns for which this ratio in the $x$ direction is also independent of position. First we show that $F$ still has a sinusoidal variation in the (infinite) $y$ direction and can therefore be written as

$$F(x,y) = G(x) \cos k_y y. \tag{16}$$

It is easier to see this if we replace $\cos k_y y$ with $\exp i k_y y$. For this complex magnetization pattern all points with the same $x$ value are equivalent except for a phase factor. Any field or charge distribution calculated for this pattern must by symmetry also have this same $y$ dependence. Thus taking the real part we see that the same must be true for the cosine distribution. This leaves us with the one-dimensional problem of determining $G(x)$. To obtain the field $H_x$ we first obtain the magnetic charge from $-S\nabla \cdot \mathbf{M}$ and then integrate to get the field (for $z=0$):

$$H_x(x,y) = SA_x \cos(k_y y) \int_0^W dx' \frac{dG(x')}{dx'} \int_{-\infty}^{\infty} dy \frac{(x-x')\cos k_y y}{[(x-x')^2 + y^2]^{3/2}}. \tag{17}$$

The $y$ integral yields an expression involving the modified Bessel function $K_1$ and the field may be expressed as

$$H_x(x,y) = SA_x \cos(k_y y)\hat{O}G(x), \tag{18}$$

where $\hat{O}$ is the integral operator

$$\hat{O}(G) = \int_0^W dx' 2k_y \mathrm{sgn}(x-x')K_1(k_y|x-x'|)\frac{d}{dx'}[G(x')]. \tag{19}$$

Appropriate solutions for $G(x)$ are therefore ones which are eigenfunctions of the operator $\hat{O}$:

$$\hat{O}G_n = \lambda_n G_n \tag{20}$$

and the corresponding ratios of the field to the magnetization are determined by the eigenvalues

$$B_x/A_x = S\lambda_n, \tag{21}$$

and this can be used in Eq. (12) to determine the mode frequency. Note that in the limit of $k_y \to 0$ the operator

reduces to

$$\hat{O}(G) = \int_0^W dx \frac{2}{(x-x')}\frac{d}{dx'}[G(x')]. \tag{22}$$

The eigenvectors and eigenvalues can be found numerically. $G(x)$ is represented by a vector, a set of $m$ evenly spaced points for $x$ from 0 to $W$. The operator becomes an $m \times m$ matrix. We are mainly interested in solutions with even symmetry because odd symmetry solutions are hidden modes that cannot be excited except by using a nonuniform rf field. This allows us to only consider points from 0 to $W/2$, which improves the accuracy of the results for a given limit on the size of the matrix. For the results we presented, $m$ was equal to 100. A standard EISPACK (Ref. 11) routine was used to calculate the eigenvalues and eigenvectors. Convergence of the lowest eigenvalues was checked by changing the value of $m$. Modes 1 and 3 (having one and three half cycles) are shown in Fig. 2. For each case we show two values of $Wk_y$: 0 and 100. The latter is about as far as we could reliably go with the calculation for large $k_y$ and appears to have con-
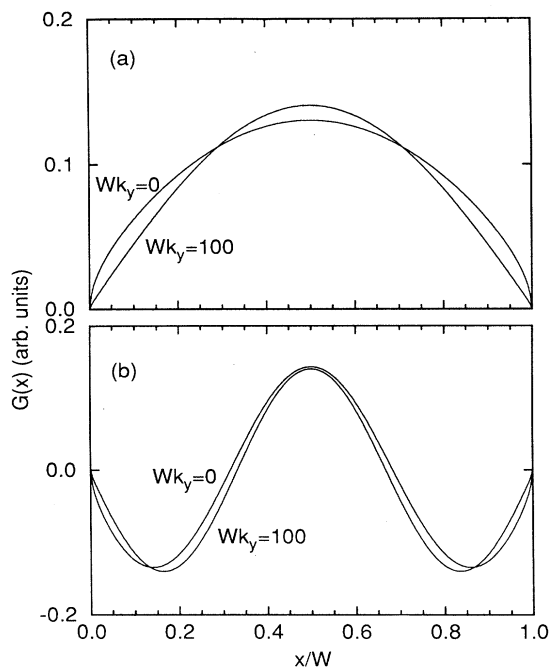
FIG. 2. Transverse $(x)$ component of the magnetization, $G(x)$, as a function of transverse position for the infinite strip (full width shown). Results are given for two values of width times longitudinal wave number, $Wk_y = 0$ and $Wk_y = 100$, as indicated. Note that for the high value of $Wk_y$ the mode pattern has converged to a sine function. The $k_y = 0$ case appears from the curvature at the center to have a lower value of $k_x$. (a) Transverse mode number $n_x = 1$. (b) Transverse mode number $n_x = 3$.

verged fairly well to a half or three half cycles of a sine function. The $k_y = 0$ case on the other hand rises more abruptly at the edges apparently with an $\sqrt{x}$ onset. One can in fact show that $\sqrt{x}$ is an exact solution for the case of a semi-infinite plane. Near the center, modes with $Wk_y = 0$ appear broader than those with $Wk_y = 100$, i.e., the ratio of the second derivative to the amplitude is smaller as though the wave number in the $x$ direction had been reduced somewhat. The corresponding eigenvalues are also smaller. We define an "effective $k$ vector" which is the value of $k_x$ which would give us the same results for the infinite plane Eq. (8) as we obtained numerically for the infinite strip. This can then be converted to an "effective mode number" which is $\pi/Wk_x$. For modes 1,
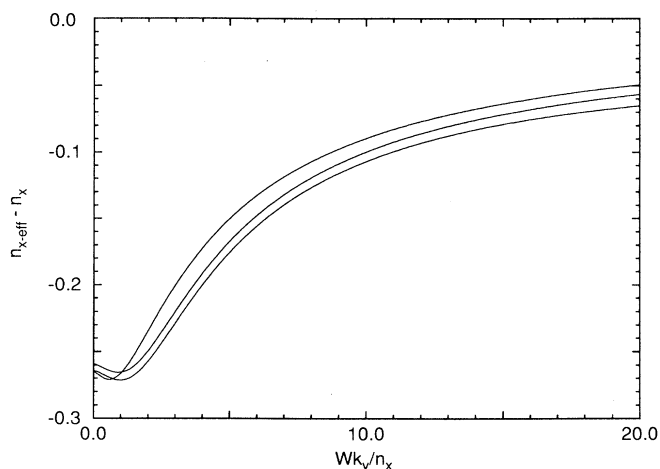


FIG. 3. Shows the deviation of the effective mode number, $n_{x\text{-eff}}$, from the actual (integer) mode number, $n_x$, as a function of longitudinal wave number for the infinite strip. Curves from top to bottom are for transverse mode numbers $n_x = 1$, 3, and 5.

3, and 5 we plot this effective mode number as a function of $Wk_y$ in Fig. 3. These curves asymptotically approach the expected integral values for large $k_y$ but start about 0.265 below this value at $k_y = 0$.

By using the effective mode number from the infinite strip when performing the calculation for the rectangular particle we can correct for edge effects. It is apparent from Fig. 3 that this will have the largest effect in the frequency of the lowest mode number (in the $x$ direction), and also that it will strongly effect the spacing between mode 1 and 3, an effect that should be noticeable even in experimental data taken at high fields where ellipticity of the precession is not significant.

## IV. NONUNIFORM DEMAGNETIZATION FIELD

In order to analyze the effects of a nonuniform demagnetizing field we consider the case of a long rectangle with the applied field $H_a$ along the long direction. If we take the magnetization to be uniform (a good approximation in this case) then the demagnetizing field can be obtained from the expression of Joseph and Schlomann.[12] Applying their Eqs. (16) and (17) to the present case, assuming that the origin is at the center of the sample, we find that the demagnetization field along the $y$ axis is

$$H_d = -4M_s \left\{ \arctan \frac{SW}{(L - 2y)\sqrt{S^2 + W^2 + (L - 2y)^2}} + \arctan \frac{SW}{(L + 2y)\sqrt{S^2 + W^2 + (L + 2y)^2}} \right\}. \quad (23)$$

Since we are still assuming that $S$ is small, the $S^2$ appearing in the square roots may be dropped. Except within a distance of order $S$ of the sample ends, the value of the argument of the arctan functions will be small and

hence the arctan will approximately equal its argument. Near the ends, the demagnetizing field rapidly increases to $-2\pi M_s$. For applied fields which are smaller than this there must be a point at which the total field becomes

negative and is opposed to the assumed direction of the magnetization. This situation is unstable, so in reality the magnetization can be expected to turn over to one side or the other in these end zones, becoming partially parallel to the edge there, possibly with the formation of domain walls. The accuracy of the results will thus be dependent on the relative size of these end zones. At any given point of the long rectangle we make the assumption that the magnetization mode pattern will assume the form of a solution to the infinite strip under the influence of the internal field $H_i = H_a + H_d$ at that point. This will mainly result in a variation of the wave number $k_y$ with position, its value decreasing as we approach the end of the sample. After reaching $k_y = 0$ we must switch over to a decaying rather than oscillatory solution. The effective $k_y$ at a given location is determined by the local curvature in the $y$ direction, i.e.,

$$k_y^2 = -\frac{d^2 F/dy^2}{F}.\qquad(24)$$

Using Eqs. (8) and (12) we obtain the following expression for $k_y^2$:

$$k_y^2 = \left[\frac{2\pi\gamma M_s S k_x^2}{\omega_x - \gamma(H_a + H_d)}\right]^2 - k_x^2.\qquad(25)$$

Substituting into the previous equation, we have a differential equation which may be solved for $F(y)$. In evaluating the expression for $k_y^2$ we will assume that $k_x$ and $\omega_x$ are approximately independent of position. The value for $k_x$ will be determined from the effective mode number obtained from the data shown in Fig. 3 using the average value for $k_y = n_y\pi/L$. In general, it may be necessary to express $\omega_x$ as a function of $H_d$:

$$\omega_x = \omega^2/(4\pi\gamma M_s + \gamma H_a + \gamma H_d).\qquad(26)$$
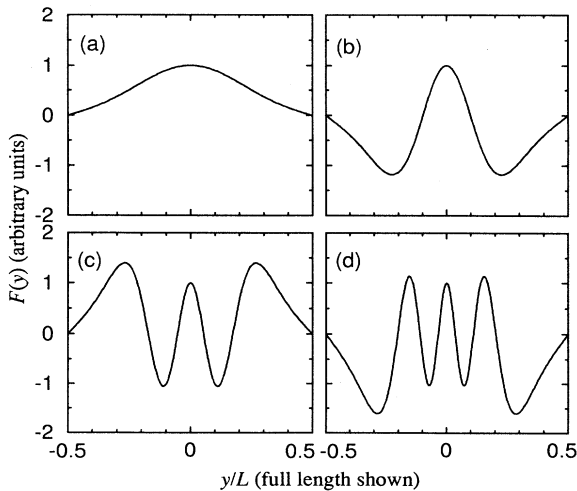


FIG. 4. Longitudinal mode patterns, $F(y)$, calculated for particles with $L/W = 3$. All have $n_x = 1$; (a), (b), (c), and (d) have $n_y = 1$, 3, 5, and 7, respectively. Note that the wave number appears to decrease on approaching the boundary in response to the stronger demagnetization field there.
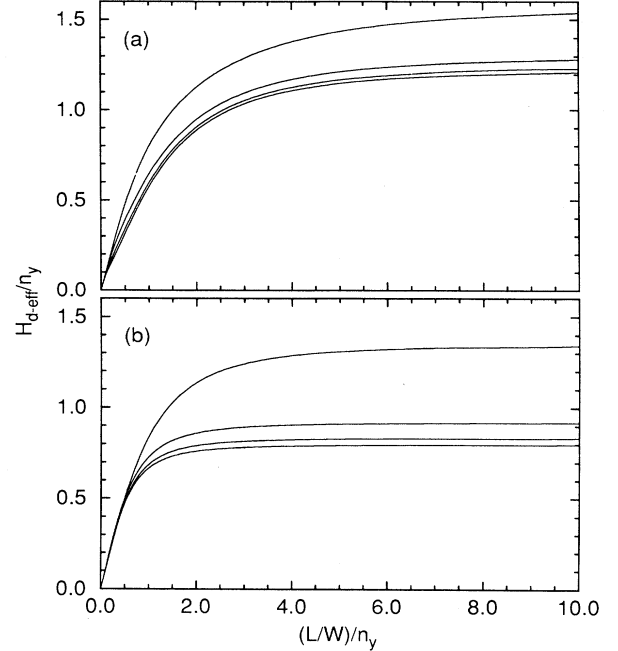


FIG. 5. Effective demagnetization factor, $H_{d\text{-eff}}$ divided by the $y$ mode number $n_y$, is given as a function of particle aspect ratio, $L/W$ divided by $n_y$, for a number of different modes. Note that the axes have been scaled (as indicated) by $1/n_y$ to show the similarity of the various curves, especially for large $n_y$. $H_{d\text{-eff}}$ is given in dimensionless units; multiply by $8WSM_s/L^2$ to obtain the field in G. (a) Curves from top to bottom are for modes $(n_y, n_x)=(1,1)$, $(3,1)$, $(5,1)$, and $(7,1)$. (b) Curves from top to bottom are for modes $(n_y, n_x)=(1,3)$, $(3,3)$, $(5,3)$, and $(7,3)$. For high-order modes, $H_{d\text{-eff}}$ tends to saturate at a level of about $n_y/\sqrt{n_x}$ for large $L/W$. The increase in proportion to $n_y$ is due to an increasing importance of the high field regions near the ends of the particle. For small $L/W$, $H_{d\text{-eff}} \approx L/W$ for all modes; however, the approximations used are not expected to be very good in this regime.

The assumption that $\omega_x$ is approximately independent of position is reasonable when $H_a$ is small compared with $4\pi M_s$, which is true for our data. Appropriate choices can be found for $\omega_x$ numerically which yield any desired mode number along the length of the sample with the boundary condition that $F = 0$ at the sample ends. Some typical mode patterns are shown in Fig. 4. As can be seen they tend to be more oscillatory in the center of the sample. This effect is less pronounced in very long samples where the demagnetization field is very weak except when very close to the ends. The effect on the frequency can be represented in terms of an effective demagnetization field for the whole sample. Values of these are plotted for several modes as a function of sample aspect ratio $L/W$ in Fig. 5.

## V. FINITE THICKNESS

In order to approximately correct for the effects of finite thickness, we will use a variational approach similar to that used by Sparks,[4] but which calculates both

$\omega_x$ and $\omega_z$ as we have done previously. This correction becomes important when the wave number in the $y$ direction starts to become comparable to the inverse thickness of the sample. The key assumption that makes this analysis possible is that we maintain the proportionality between the magnetization and the field in the $x$ and $z$ directions as we have had previously. This is for the applied field along the $y$ axis as has been our previous assumption. For the applied field along the $x$ or $z$ axis a similar relation is also required for the field and magnetization in the $y$ direction, so that

$$h_x = \lambda_x m_x, \tag{27}$$

$$h_y = \lambda_y m_y, \tag{28}$$

$$h_z = \lambda_z m_z, \tag{29}$$

where the $\lambda$'s are all approximate constants to be determined, and the other variables are all proportional to some function $F(x, y, z)$. In this case, linearizing the gyromagnetic equation [Eq. (9)] and assuming $\exp(i\omega t)$ time dependence, one can obtain

$$\hat{A}_z m_z = -i\omega m_x, \tag{30}$$

$$\hat{A}_x m_x = i\omega m_z, \tag{31}$$

where $\hat{A}_x$ and $\hat{A}_z$ are the operators which include effects of the internal dc field $H_i$, the exchange field, and the ac demagnetizing field:

$$\hat{A}_x = \gamma \left( H_i - D\nabla^2 - M_s \frac{\partial}{\partial x} \int dr' \frac{1}{|\mathbf{r} - \mathbf{r}'|} \frac{\partial}{\partial x} \right), \tag{32}$$

$$\hat{A}_z = \gamma \left( H_i - D\nabla^2 - M_s \frac{\partial}{\partial z} \int dr' \frac{1}{|\mathbf{r} - \mathbf{r}'|} \frac{\partial}{\partial z} \right), \tag{33}$$

where $D$ is the exchange constant, $D \approx 3.15 \times 10^{-9}$ G cm$^2$ for Permalloy. As can be seen by multiplying Eqs. (30) and (31) together, the variational expression for the frequency which corresponds to Sparks[4] Eq. (8) is given by

$$-\omega^2 = \langle \hat{A}_x \hat{A}_z \rangle_{m_x m_z} = \langle \hat{A}_x \rangle_{m_x} \langle \hat{A}_z \rangle_{m_z}, \tag{34}$$

where we define

$$\langle \hat{A} \rangle_m = \int dr\, m^* Am \bigg/ \int dr\, m^* m. \tag{35}$$

We will naturally choose the same trial function $\tilde{m}(x, y, z)$ for the magnetization pattern in any direction required ($x$ and $z$ in the present case of $H_a$ along $y$). Surface pinning effects may be important in very thin samples, but we neglect this effect here and assume $\tilde{m}$ is independent of $z$. For odd modes, with the origin at the center of the sample, we assume the trial function

$$\tilde{m} = \cos(k_x x) \cos(k_y y). \tag{36}$$

For this trial function we find for the exchange frequency

$$\omega_e = \langle -\gamma D\nabla^2 \rangle = \gamma D(k_x^2 + k_y^2). \tag{37}$$

We can obtain average values for the $\lambda$'s:

$$\lambda_x = \left\langle \frac{\partial}{\partial x} \int dr' \frac{1}{|\mathbf{r} - \mathbf{r}'|} \frac{\partial}{\partial x} \right\rangle, \tag{38}$$

$$\lambda_y = \left\langle \frac{\partial}{\partial y} \int dr' \frac{1}{|\mathbf{r} - \mathbf{r}'|} \frac{\partial}{\partial y} \right\rangle, \tag{39}$$

$$\lambda_z = \left\langle \frac{\partial}{\partial z} \int dr' \frac{1}{|\mathbf{r} - \mathbf{r}'|} \frac{\partial}{\partial z} \right\rangle. \tag{40}$$

Using the same approximations which Sparks[4] used to obtain his Eq. (26), we obtain

$$\lambda_x = -4\pi Q k_x^2 / k_f^2, \tag{41}$$

$$\lambda_y = -4\pi Q k_y^2 / k_f^2, \tag{42}$$

$$\lambda_z = -4\pi (1 - Q), \tag{43}$$

where

$$Q = 1 - (1 - e^{-k_f S}) / k_f S \tag{44}$$

and

$$k_f = \sqrt{k_x^2 + k_y^2}. \tag{45}$$

Note that $\lambda_x + \lambda_y + \lambda_z = -4\pi$, which is the same as for static demagnetization factors in an ellipsoid. Note also that for $k_f S \ll 1$, $Q \approx k_f S/2$, in which case the results above reduce to those obtained previously for the infinite plane, see Eqs. (6) and (8). Using the above expressions we obtain an expression for the frequency for $H_a$ parallel to the $y$ axis:

$$\omega^2 = (\gamma H_i + \omega_e + \gamma M_s \lambda_x)(\gamma H_i + \omega_e + \gamma M_s \lambda_z). \tag{46}$$

## VI. COMPARISON OF EXPERIMENT AND THEORY

Equation (46), our most general result, is evaluated and compared to our experimental data in Table I. Quite good agreement is obtained when this final form is used with the effective transverse mode number and effective demagnetization field, as obtained from Figs. 3 and 5 (compare $H_{cor}$ and $H_{exp}$).

TABLE I. Data for rectangular Permalloy particles, with $x$, $y$, and $z$ dimensions of 1 $\mu$m, 3 $\mu$m, and 0.0735 $\mu$m and with the dc field applied along the $y$ axis. Comparison of the experimentally observed resonance field, $H_{expt}$ (see Fig. 1), with the value calculated by the infinite plane approximation, $H_{inf}$ [see Eq. (14)], and with the value obtained from the corrected variational method, $H_{cor}$ [see Eq. (46)], in which we used the effective $x$ mode number $n_{x\text{-eff}}$ and the result was increased by the magnitude of the effective demagnetization field $H_{d\text{-eff}}$.

| $n_y, n_x$ | $n_{x\text{-eff}}$ | $H_{d\text{-eff}}$ | $H_{inf}$ | $H_{cor}$ | $H_{expt}$ |
|---|---|---|---|---|---|
| 1,1 | 0.73 | -73 | 34 | 533 | 520 |
| 3,1 | 0.80 | -100 | 286 | 766 | 751 |
| 5,1 | 0.85 | -102 | 489 | 967 | 911 |
| 7,1 | 0.89 | -99 | 615 | 1095 | 1034 |
| 9,1 | 0.91 | -95 | 698 | 1200 | 1128 |
| 11,1 | 0.92 | -91 | 754 | 1288 | 1202 |
| 13,1 | 0.93 | -88 | 794 | 1361 | 1273 |
| 15,1 | 0.94 | -85 | 825 | 1426 | 1330 |
| 17,1 | 0.95 | -83 | 848 | 1479 | 1382 |

TABLE II. Data for rectangular Permalloy particles, with $x$, $y$, and $z$ dimensions of 0.5 $\mu$m, 1.5 $\mu$m, and 0.0735 $\mu$m and with the dc field applied along the $y$ axis. Comparison of the experimentally observed resonance field, $H_{\text{expt}}$, with the value calculated by the infinite plane approximation, $H_{\text{inf}}$ [see Eq. (14)], and with the value obtained from the corrected variational method, $H_{\text{cor}}$ [see Eq. (46)], in which we used the effective $x$ mode number $n_{x\text{-eff}}$ and the result was increased by the magnitude of the effective demagnetization field $H_{d\text{-eff}}$. Inaccuracy of $H_{\text{cor}}$ for the first few modes is likely due to the nonuniformity of the magnetization caused by the low value of the internal field for these modes. Note that the calculated internal field, $H_{\text{cor}} + H_{d\text{-eff}}$, is negative for the first mode.

| $n_y,n_x$ | $n_{x\text{-eff}}$ | $H_{d\text{-eff}}$ | $H_{\text{inf}}$ | $H_{\text{cor}}$ | $H_{\text{expt}}$ |
|---|---|---|---|---|---|
| 1,1 | 0.73 | -146 | -946 | 134 | 372 |
| 3,1 | 0.80 | -200 | -450 | 639 | 788 |
| 5,1 | 0.85 | -204 | -50 | 989 | 1074 |
| 7,1 | 0.89 | -198 | 201 | 1221 | 1255 |
| 9,1 | 0.91 | -190 | 364 | 1392 | 1388 |
| 11,1 | 0.92 | -181 | 476 | 1515 | 1487 |

If the microwave frequency is too low for a particular geometry of particle it is possible for the calculation to yield a negative value for the internal dc field $H_i$. In such cases, a resonance may still be observed experimentally but shifted to a somewhat higher field due to a considerable amount of domain structure formed in response to the low applied field. Such is the case for the data in Table II taken from particles which are 0.5 $\mu$m $\times$1.5$\mu$m $\times$0.0735 $\mu$m. The (1,1) mode has the lowest resonance field and is most strongly effected; agreement improves rapidly for the higher modes.

Other orientations of the dc field may also be used. In Table III we have applied the field along the 1 $\mu$m direction of the array of 1 $\times$ 3 $\mu$m particles. Although a number of approximations which we are using are not particularly applicable for this orientation, we can still do a fair job of predicting the observed frequencies.

Table IV shows experiment and theory for the dc field applied perpendicular to the surface of this same array of particles. In this case we can obtain effective mode numbers for both the $x$ and $y$ directions since these are both orthogonal to the applied field. The demagnetization field is much larger now than it was for the cases

TABLE III. Data for rectangular Permalloy particles, with $x$, $y$, and $z$ dimensions of 3 $\mu$m, 1 $\mu$m, and 0.0735 $\mu$m and with the dc field applied along the $y$ axis. Comparison of the experimentally observed resonance field, $H_{\text{expt}}$, with the value calculated by the infinite plane approximation, $H_{\text{inf}}$ [see Eq. (14)], and with the value obtained from the corrected variational method, $H_{\text{cor}}$ [see Eq. (46)], in which we used the effective $x$ mode number $n_{x\text{-eff}}$ and the result was increased by the magnitude of the effective demagnetization field $H_{d\text{-eff}}$.

| $n_y,n_x$ | $n_{x\text{-eff}}$ | $H_{d\text{-eff}}$ | $H_{\text{inf}}$ | $H_{\text{cor}}$ | $H_{\text{expt}}$ |
|---|---|---|---|---|---|
| 1,1 | 0.91 | -457 | 921 | 1505 | 1312 |
| 3,1 | 0.96 | -456 | 993 | 1735 | 1612 |
| 5,1 | 0.98 | -452 | 1009 | 1888 | 1775 |

TABLE IV. Data for rectangular Permalloy particles, with $x$, $y$, and $z$ dimensions of 1 $\mu$m, 3 $\mu$m, and 0.0735 $\mu$m and with the dc field applied along the $z$ axis. Comparison of the experimentally observed resonance field, $H_{\text{expt}}$, with the value obtained from the corrected variational method, $H_{\text{cor}}$ [see Eq. (46)], in which we used the effective $x$ and $y$ mode numbers, $n_{x\text{-eff}}$ and $n_{y\text{-eff}}$, and the result was increased by the magnitude of the demagnetization field at the center of the particle, $H_d \approx -9557$ G.

| $n_y,n_x$ | $n_{y\text{-eff}}$ | $n_{x\text{-eff}}$ | $H_{\text{cor}}$ | $H_{\text{expt}}$ |
|---|---|---|---|---|
| 1,1 | 0.905 | 0.735 | 12518 | 12400 |
| 3,1 | 2.79 | 0.804 | 12287 | 12225 |
| 5,1 | 4.74 | 0.854 | 12055 | 12034 |
| 7,1 | 6.74 | 0.885 | 11856 | 11875 |
| 9,1 | 8.74 | 0.905 | 11689 | 11675 |

where the dc field was in the plane of the film. In calculating the corrected resonance field $H_{\text{cor}}$ we use the value of the field at the center of the particle which is given by[9]

$$H_d \approx -4\pi M_s(1 - 2S\sqrt{L^2 + W^2}/\pi LW). \qquad (47)$$

For the 1$\times$3$\times$0.0735 $\mu$m particles we obtain $H_d \approx -4\pi M_s \times 0.9507 = -9557$ G. The field is relatively constant in the middle of the particle, but falls off rapidly when within a distance of about $S$ from an edge; thus the effective demagnetization field will be slightly lower in magnitude than the value obtained above and may also depend on which mode is being excited.

## VII. CONCLUSION

We have discussed in detail a number of factors which influence the frequency and mode pattern for rectangular ferromagnetic particles. This work includes the theoretical behavior of an infinite strip of finite width and negligible thickness which has not been studied previously. We have discussed the effects of finite length and the associated nonuniform demagnetization field, which leads to a position dependent wave number for the mode along this direction. We have also studied the effects of finite thickness using a variational approach similar to one used previous by Sparks.[4] Our most general theoretical result given in Eq. (46) gives very good agreement with our experimental results as was shown in Sec. VI.

*Present address: Department of Physics, University of California, Santa Barbara, CA 93106.

[1] L. R. Walker, Phys. Rev. **105**, 390 (1957).

[2] R. W. Damon and J. R. Eshbach, J. Phys. Chem. Solids **19**, 308 (1961).

[3] P. C. Fletcher and C. Kittel, Phys. Rev. **120**, 2004 (1960).

[4] M. Sparks, Phys. Rev. B **1**, 3831 (1970).

[5] B. E. Storey, A. O. Tooke, A. P. Cracknell, and J. A. Przystawa, J. Phys. C **10**, 875 (1977).

[6] J. F. Smyth, S. Schultz, D. R. Fredkin, D. P. Kern, S. A. Rishton, H. Schmid, M. Cali, and T. R. Koehler, J. Appl. Phys. **69**, 5262 (1991).

[7] C. Warren and H. B. Callen, in *Magnetism Volume I*, edited by G. T. Rado and H. Suhl (Academic, New York, 1963), p. 540.

[8] M. Sparks, B. R. Tittman, J. E. Mee, and C. Newkirk, J. Appl. Phys. **40**, 1518 (1969).

[9] J. Barak, J. Appl. Phys. **63**, 5830 (1988).

[10] J. Barak and U. Lachish, J. Appl. Phys. **65**, 1652 (1989).

[11] B. T. Smith *et al.*, *Matrix Eigensystem Routines:* EISPACK *Guide*, 2nd ed. (Springer, New York, 1976).

[12] R. I. Joseph and E. Schlomann, J. Appl. Phys. **36**, 1579 (1965).